Article

Forensic Investigations of Geohazards: The Norcia 2016 Earthquake

Pier Matteo Barone [1,2,*] and **Rosa Maria Di Maggio [2]**

[1]   American University of Rome, Archaeology and Classics Program, Via Pietro Roselli 4, I-00153 Rome, Italy
[2]   Geoscienze Forensi Italia®-Forensic Geoscience Italy, Viale Mediterraneo 77, I-00122 Rom , Italy;
      dimaggio@geologiaforense.com
[*]   Correspondence: p.barone@aur.edu

check for updates

Abstract: Earthquakes represent one of the world's most significant hazards in terms of damage to human and animal life, and property. Earthquakes also cause many other related fatalities and damage to urban structures. This paper presents the forensic investigation of failures induced by the Norcia 2016 earthquake in Italy. The detailed geophysical field investigations were carried out at selected locations in two cities: Rome and Amelia. The places of investigation were 150 km and 90 km, respectively, from the epicenter. A ground penetrating radar (GPR) survey was carried out at the sites to highlight structural failures, and included a partially damaged urban bridge, and the cracked wall of a private house. These failures have been discussed with reference to the field measurements carried out. In both cases, the GPR radargram showed clear lesions along with their geometry and location. This forensic geoscientific analysis highlights the importance of detecting structural damage immediately after a geohazard event to help plan proper interventions, efforts to prevent human losses and help law enforcement to focus their forensic investigations.

Keywords: forensic geoscience; forensic geophysics; GPR; geohazard; earthquake

1. Introduction

The importance of non-destructive techniques such as the ground penetrating radar (GPR) is well known across various fields of its application. In particular, this methodological approach is often used in forensics to help investigators locate bodies or stolen objects that are buried ([1], and the literature therein). Moreover, this tool is frequently used in geological research and risk studies as it allows mapping of the subsoil, its stratigraphy, and its critical points in an accurate and completely non-invasive manner [2–5]. When geological risk is intertwined with forensic investigation, we refer to it as a forensic geohazard.

In fact, the use of this geophysical method, GPR, has been recently developed in interconnected environments where several major natural catastrophes (such as earthquakes, floods, landslides, etc.) unfortunately lead to deaths and/or structural damage [6–11]. In this context, GPR can play a key role not only in the search for missing persons [12], but also in the monitoring of possible damage to structures and buildings.

Adequate prevention of damage caused by natural disasters requires improving the level of knowledge of buildings, and detecting structural and non-structural anomalies and vulnerabilities that need to be corrected urgently [13]. In the first place, a geometric-structural survey is used to represent the overall geometry of the constructive elements, while also considering the state of conservation of the materials and the lesions (in progress or stable) through identification of the fractures and damage. Fractures in an existing building, depending on the type of the fractures and the circumstances, can be warning signals. Therefore, when analyzing fractures, it is essential to understand whether they are

due to settling of the structure or due to a more serious phenomenon that could lead to the collapse of the load-bearing elements ([14,15], and literature therein).

In a given area and within a given time interval, the seismic risk can be measured by the extent of damage that is expected because of earthquakes. The hazard can be assessed in terms of victims, economic loss, and damage to buildings. Hazards and risks have the same relationship as cause and effect; in fact, risk is represented by the earthquake (the cause) that can strike a certain area, while hazard is represented by its possible consequences, that is, by the damage that can be expected (the effect) [16]. The definition of hazard is influenced not only by the risk, but also by the characteristics of the territory. In order to define the hazard level of a territory, it is necessary to know the territorial seismicity, that is, the frequency of earthquakes and their intensity, the method of construction of the structures, the quantity and quality of the exposed goods, and the density of the population [17]. Considering the same frequency and intensity of earthquakes, the hazard is zero where there are no buildings, exposed goods or population, while on the other hand, densely populated areas or areas characterized by structures that are not resistant to the shaking by a seismic wave represent a high level of hazard [18,19].

The forensic aspect of non-destructive geoscientific investigations lies in its ability to help in rapidly identifying, and thereby, preventing further post-shake collapses and possible victims, in particular in Italy where this approach is not common.

This last aspect, together with an analysis of the structures, will be discussed in detail in the following sections. The study not only tested the GPR's ability to monitor and identify damage during the seismic event known as Norcia 2016, in Italy, in urban areas and densely inhabited places several kilometers away from the epicenter, but also evaluated the logistical contribution that this method can make to law enforcement in preventing post-earthquake damage by reducing collapses [20].

2. Materials and Methods

The areas under investigation were in the cities of Amelia (in the province of Terni) and Rome, 90 km and 150 km away from the epicenter of the earthquake in Norcia (Italy), respectively. The places in which the GPR surveys were conducted included: (i) a private house in the center of Amelia, and (ii) the Marconi Bridge—one of the busiest bridges in Rome, located on the River Tiber (Figure 1).

Figure 1. The epicenter of the Norcia 2016 earthquake and the two areas in which the GPR investigations were performed (source: Google Earth).

2.1. The Norcia 2016 Earthquake

The earthquake that struck Italy on 30 October 2016, at 06:40:17 UTC, (07:40:17, Italian time) was the strongest earthquake since the 1980 Irpinia earthquake. The hypocenter lay at Latitude 42.84 North, Longitude 13.11 East, and at a depth of 9 km. The magnitude calculated in the Istituto Nazionale di Geofisica e Vulcanologia (INGV) monitoring room was 6.1 ML and 6.5 MW as compared to the 6.9 MW of the Irpinia earthquake. The earthquake affected the provinces of Perugia, Rieti and Macerata and was strongly felt in Central Italy; the epicenter was located 5 km from Norcia, 7 from Castelsantangelo sul Nera and Preci, and 10 km from Visso. In case of an earthquake of magnitude 6.5, the fault has an area of several hundred square kilometers and, therefore, the entire area above and around the fault is affected by strong shaking. The earthquake of 30 October was the strongest event of a sequence which began with an earthquake on 24 August of 6.0 MW and another earthquake of 26 October of the magnitude MW = 5.9 [21–27].

The Italian Accelerometric Network (RAN), managed by the Department of Civil Protection (DPC), and the Italian Seismic Network, managed by the Istituto Nazionale di Geofisica e Vulcanologia (INGV) provided the records of about 650 accelerometric stations. In Figure 2, thanks to both the Italian strong-motion database, ITACA (Italian Accelerometric Archive (http://itaca.mi.ingv.it)) and the USGS database (http://earthquake.usgs.gov), it is possible to calculate the peak ground acceleration (PGA) at the epicenter and at the two study areas (Amelia and Rome). These were 536.48, 18.28, and 24.29 cm/s^2, respectively [23–25].
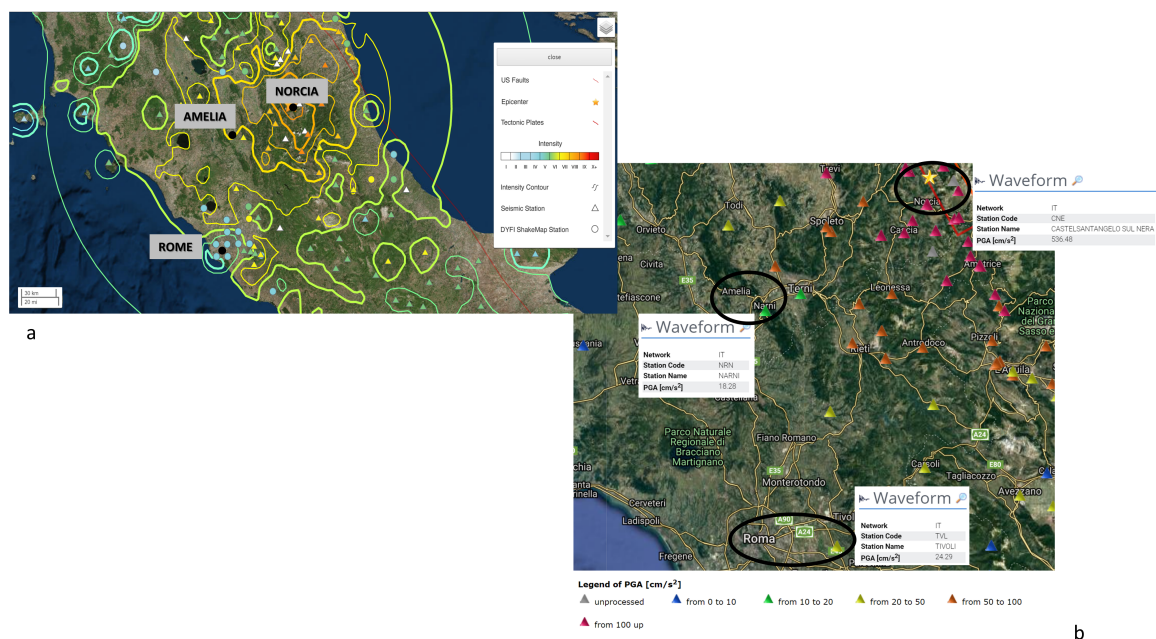

Figure 2. (**a**) The intensity of the Norcia 2016 earthquake (source USGS: http://earthquake.usgs.gov); (**b**) The peak ground acceleration (PGA) relative to the two study areas and the epicenter (source ITACA: http://itaca.mi.ingv.it).

2.2. The GPR Measurements

Over the last thirty years, geophysical techniques have been increasingly used to detect the presence of anomalies in the subsurface, as well as to estimate the hidden targets inside the walls of a building. Geophysical methods can be effectively applied to produce an image of a buried target to prevent extensive, destructive, time consuming and expensive excavations [28].

The scope of a geophysical measurement is the detection of the "boundaries" between objects having different values of a specific physical property. The contrast between the searched target and the background should be strong enough to be detected "at a distance". That is, the target should

be able to generate a measurable relative spatial variation of the specific physical property at the surface [29].

GPR operates at frequencies between a few MHz and 3 GHz. GPR's depth of penetration depends on the electrical properties of the ground. For example, in the case of ground with a relatively high conductivity (such as caused by saturated clay), the depth of penetration may be less than 0.5 m, yet in the case of quartz sand, which has low conductivity, GPR penetration may be tens of meters [30].

The radar unit produces a pulsed electromagnetic wave that travels through the ground at a velocity controlled by the electrical properties of the subsurface. Differences in relative permittivity (dielectric constant) or electrical conductivity due to changes in soil/material type or water chemistry result in the waves being reflected. By moving the radar antenna over the material surface, a continuous real-time section (radargram) is built up by arranging each radar record next to the other. The horizontal axis of the section represents the distance (m), and the vertical axis represents the two-way travel times (TWT) of reflections in nanoseconds (ns). To transform this information into distance, the velocity must be known. The lines shown on the radargram represent reflectors and are constructed of coalescing wiggle traces from individual radar records [31,32].

For most survey reports, grayscale plots of the radargrams (i.e., GPR sections or B-scans) are the primary presentation format, and several improvements have been introduced to create a more solid appearance. If one has collected multi-profile grids, one can develop maps (i.e., time/depth slices or C-scans) representing various depths by using the average envelope amplitude and by interpolating among all of the radargrams [33].

In this work, the GPR used in both measurements was the bistatic FINDAR (Sensors & Software, Inc. Mississauga, ON, Canada) system, equipped with a 500 MHz antenna.

In the private apartment in Amelia, a visibly damaged wall was analyzed to understand the internal geometry of the fracture that was assumed to pass through the masonry from the inner part of the apartment to the outer part, which was on the balcony. This type of investigation is well documented in the literature [34–40], but less used in the post-earthquake situation. The whole house was built in the 1970s, before the new anti-seismic rules and before the modern development of the seismic vulnerability map. The building is a hybrid structure, masonry and reinforced concrete, and this was the most evident and critical crack.

Data was acquired vertically inside a 1.1 m × 1.2 m one-way grid, with a distance of 0.1 m among profiles (Figure 3). No other processing beyond the standard one (AGC, DeWOW and Average Envelope Amplitude) was required. The signal penetration velocity was calculated using the hyperbola calibration and verified using the actual measurements of the exposed masonry: 0.14 m/ns.

On the Marconi Bridge in Rome, the GPR investigation was focused on the pavements of the bridge. This bridge was built between 1937 and 1955; the construction was interrupted due to the WWII and was only resumed in 1953. The total length is about 235 m and it is the longest bridge in Rome, with six arches and a width of about 31 m [41]. It has a "winged" structure where the central part of the bridge, supported by the pylons, is crossed by vehicles, while the external "wings" are the sidewalks (Figures 4 and 5). This type of investigation is also well known in the literature [34,42–45]; however, there has been little post-seismic application, especially in bridges having this particular structure.

Figure 3. (**a**) The crack in the masonry and the dimension of the one-way grid; (**b**) shows a similar crack in the same wall in the balcony.

Figure 4. The Marconi Bridge on the River Tiber within the urban context of Rome (**a,c**); (**b**) The beginning of its construction after WWII (source: Google Earth).
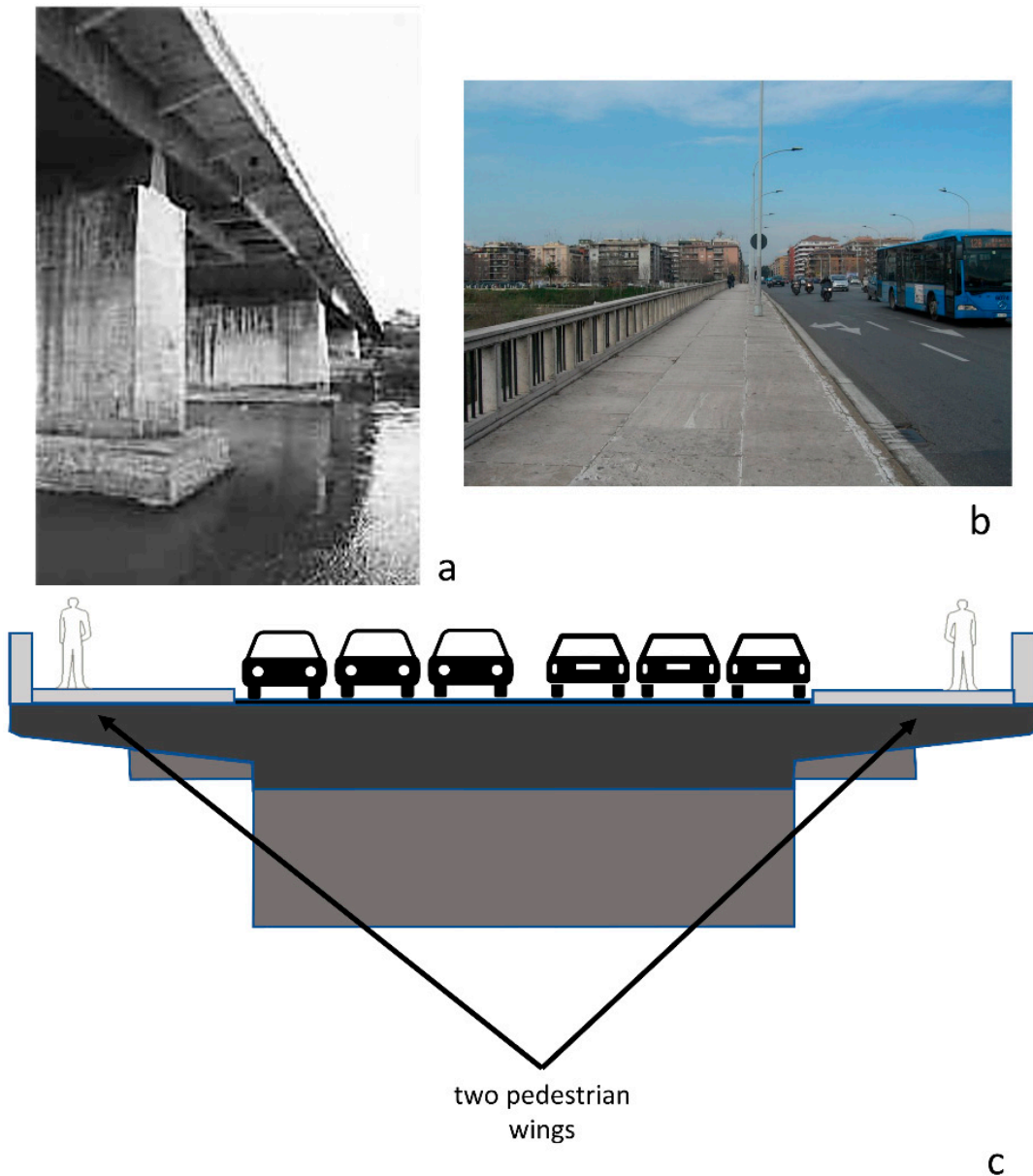
Figure 5. (**a**) The "winged" structure of the Marconi Bridge; (**b**) Note the difference between the sidewalk (covered by travertine) and the road (covered by the asphalt); (**c**) Schematic illustration of a section of the Marconi Bridge.

We acquired both single profiles along the two sidewalks, above the "wings", where the greatest damage and detachments were visible after the 2016 earthquake (Figure 6), and one-way grids of 5 m × 3 m, with a distance of 0.25 m between the profiles in the most severely damaged areas. No processing beyond the standard processing (AGC, DeWOW and Average Envelope Amplitude) was required. The signal penetration velocity was calculated by means of the calibration of the hyperboles, and subsequently verified by the real measurements of the thickness of the visible wings. It was 0.14 m/ns.

Figure 6. The visible detachments along the sidewalk of Marconi Bridge after Norcia 2016 earthquake (**a**,**b**).

3. Results and Discussion

GPR, a technologically advanced tool, proved to be a suitable solution to the problem of monitoring structures with visible damage caused by catastrophic events, such as this earthquake and the resulting geohazards in the post-seismic phase.

As for the private house in Amelia, the damage to the masonry can be easily related to the earthquake of 2016, because the crack was not present before the earthquake. In the case of the Marconi Bridge, the request for monitoring the internal structure came following the detachments (see Figure 5) that were discovered after the 2016 earthquake. The main findings of the two investigated areas have been reported below.

3.1. Amelia

Figure 7 shows the single profile acquired inside the above-mentioned grid and the depth-slices that clearly illustrate the presence of an oblique anomaly, which probably corresponds with the fracture visible on the masonry. It is worth noticing that this fracture passes through the masonry from side to side, to affect the outer wall of the room, also on the balcony side. The last slice in Figure 8, acquired from inside the room at about 0.5 m depth coincides in shape and geometry with the fracture visible outside on the balcony. Thanks to the penetration capacity and the resolution of the GPR, it was possible to understand not only the internal geometry of the fracture but also its gravity, and it facilitated the restructuring that prevented the collapse of the wall and the possible damage to property and people. Given its sudden appearance of this crack following the Norcia 2016 earthquake and its peculiar nature it is also closely related to the similar post-seismic damage found in the area in other buildings [46].
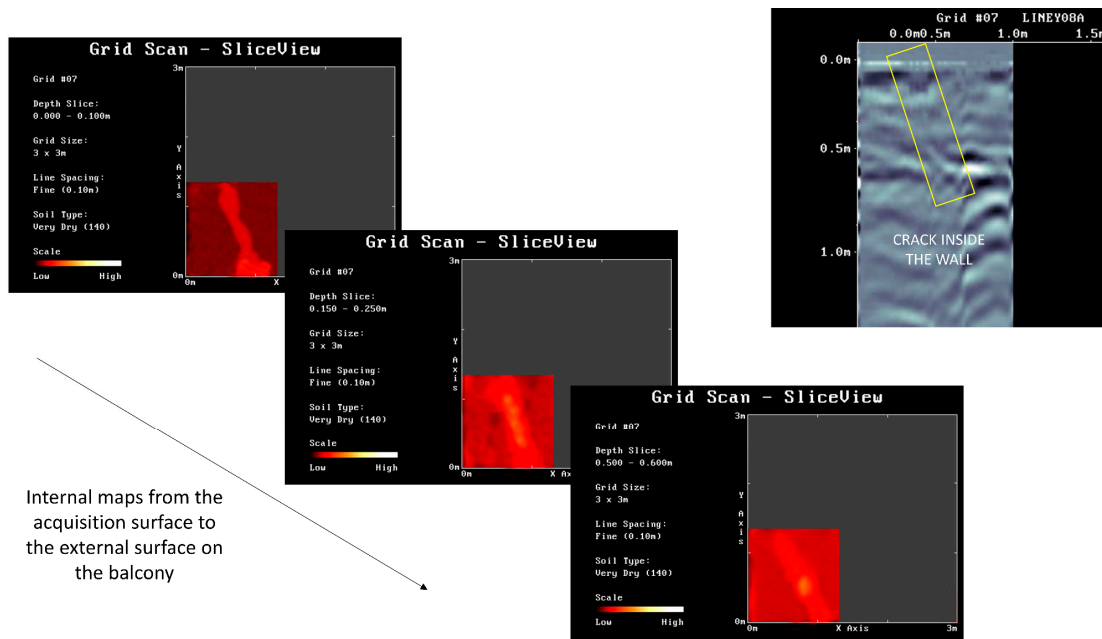
Figure 7. Both the GPR profiles (top right) and the three depth-slices show the presence of the crack and its inner geometry passing through the 0.5 m thick masonry from side to side.
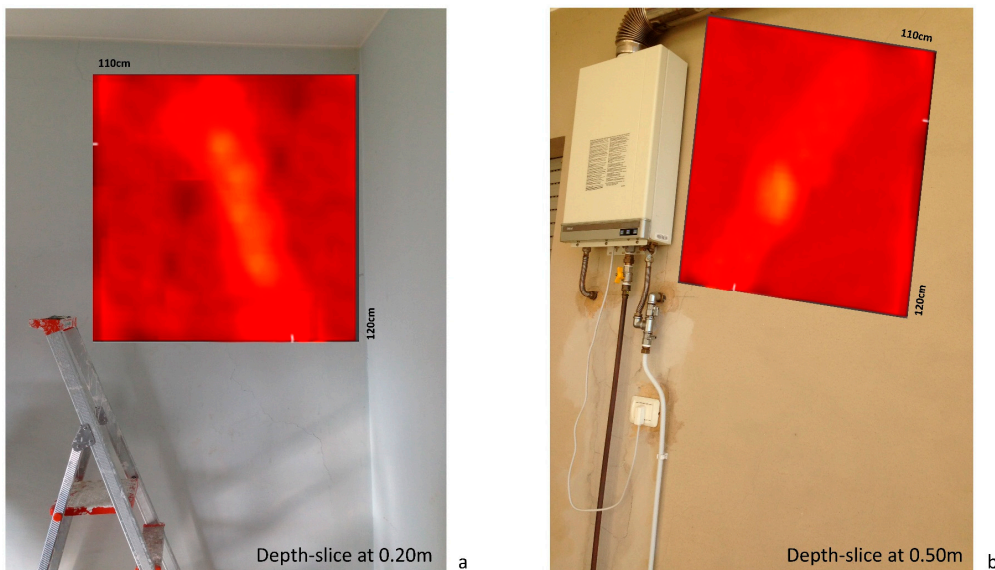

Figure 8. (**a**) The depth-slice at 0.2 m inside the masonry, revealing its inner geometry; (**b**) The depth-slice at 0.5 m of the same crack in the wall from the balcony.

3.2. Rome

Figure 9 shows the orientation of the profiles acquired along the two "wings" of the Marconi Bridge, and the attempt to overlap one of the GPR profiles to show the thickness of these "wings" and the penetration of the radar signal through the pylons up to the surface of the river water below. Figure 10 shows in detail the most obvious anomalies found from the acquired images. If, on the one hand, the thickness of the "wings" at about 0.6 m is clear, on the other hand, there are evident inconsistent hyperbolic events that can only be traced back to the presence of detachments or cracks inside the sidewalks, as partially shown in Figure 6. Moreover, the detected GPR anomalies are near these visible lesions on the bridge.
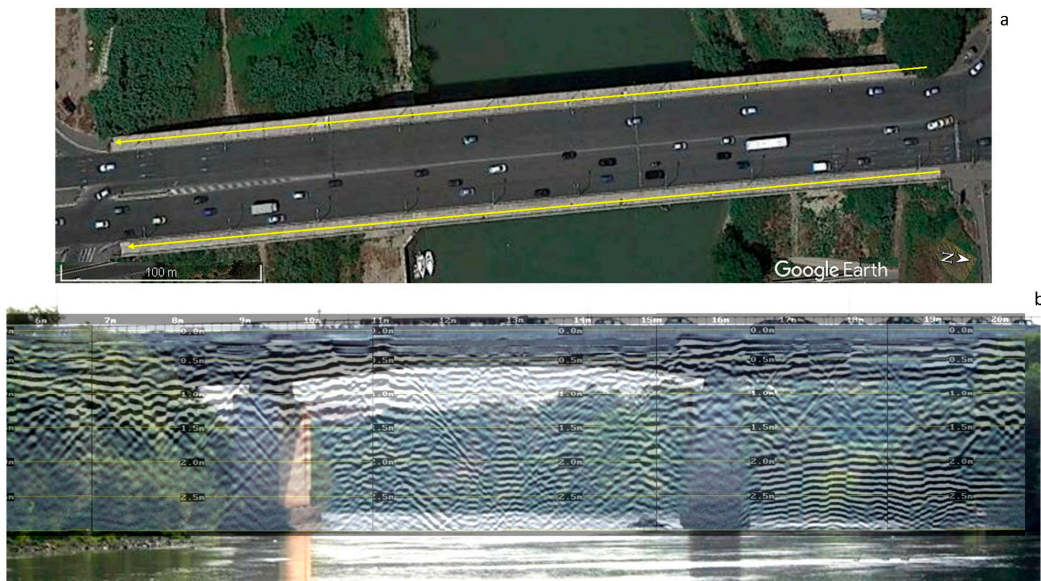
Figure 9. (**a**) The orientation of the profiles acquired along the two "wings" of the Marconi Bridge (Google Earth image); (**b**) is an overlap attempted to show a GPR profile showing the thickness of the "wings" and the penetration of the radar signal through the pylons and up to the surface of the river water below.
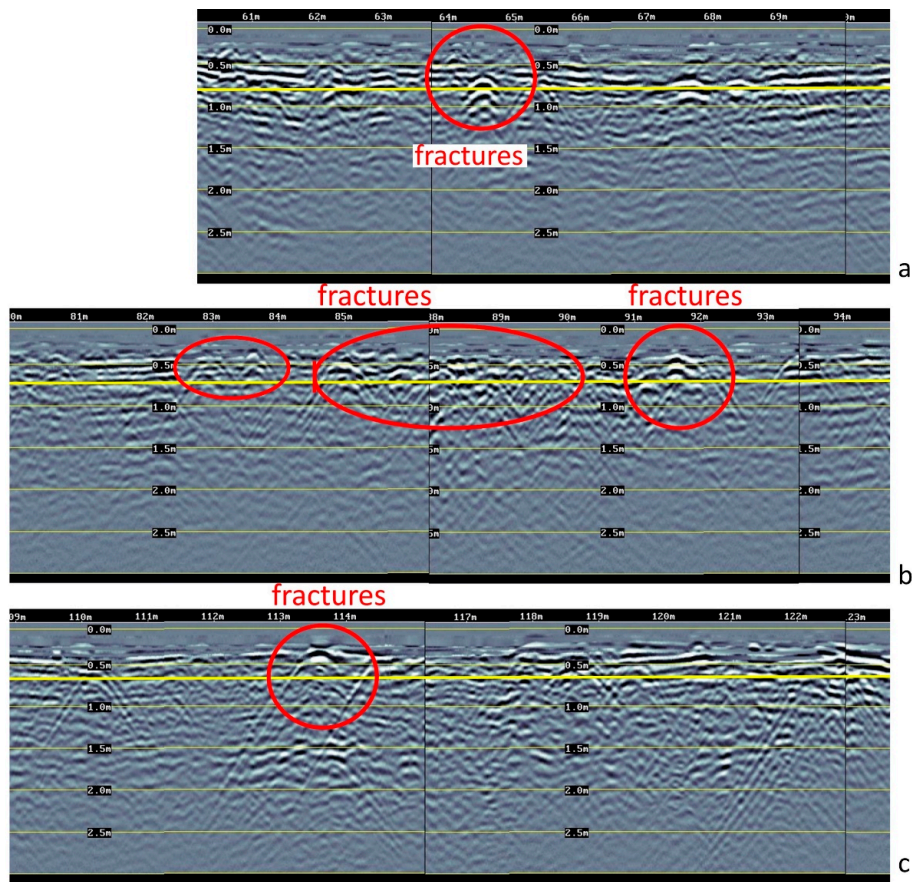

Figure 10. (**a**–**c**) show in greater detail the most obvious anomalies found close to the visible damaged part of the bridge (Figure 6). The yellow portion clearly shows the thickness of the wings at about 0.6 m.

In addition to the internal damage to the "winged" structure of the bridge, there are also more superficial damage linked to the failure of the travertine surface that covers the sidewalks. This is evident from Figure 11, where both the radar profiles and the depth-slices show evident anomalies due to detachments and lesions.
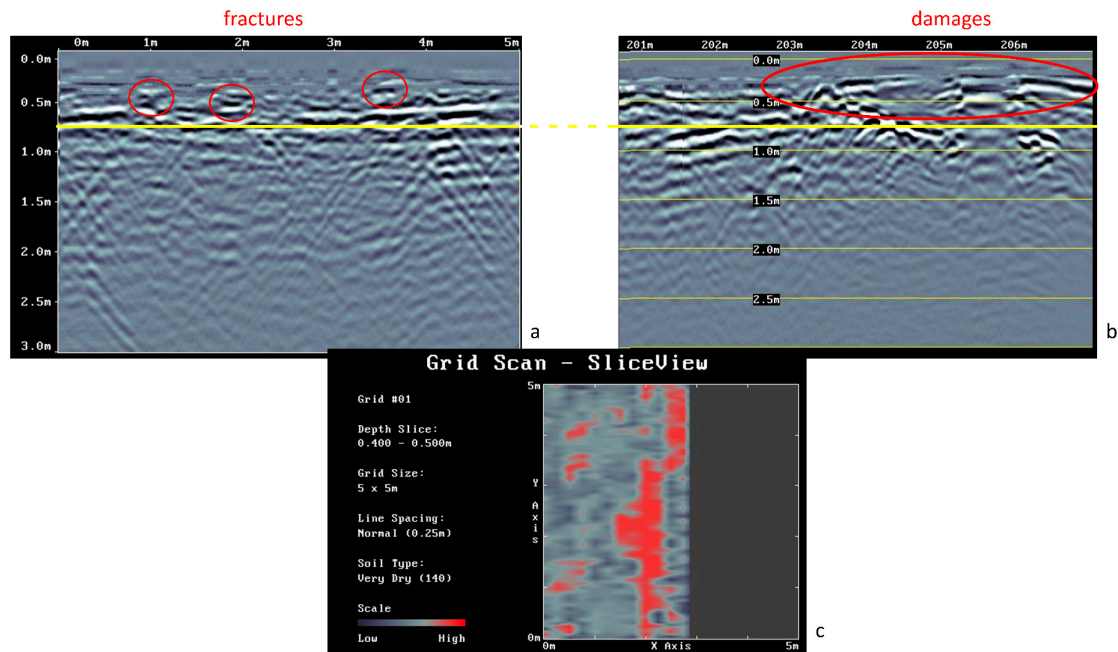

Figure 11. (**a**) Illustrates the internal damage to the "winged" structure of the bridge; (**b**) Shows superficial damage linked to the failure of the travertine surface of the sidewalks; (**c**) highlights the depth-slices showing evident anomalies due to detachments and cracks (in red).

Note that, although the cracks illustrated in Figure 5 are certainly post-2016 earthquake and Rome suffered similar damage after this seismic event [47,48], the other injuries highlighted by the GPR surveys are not due to this shaking alone.

The use of geoscientific solutions such as GPR for structural monitoring of delicate buildings, infrastructure, etc. in a post-earthquake context, is the basis of any forensic preventive action aimed at improving the control of the territory, geohazards, and its resilience to catastrophic events, and preventing collateral damage to property and people. Non-destructive methods, such as the one used in this work, have identified every single element of the damage suffered by or the cracking in the investigated structures. Thanks to a targeted and timely intervention, the critical points can be flagged in real time.

4. Conclusions

The necessity to control the territory affected by catastrophic events, such as earthquakes is now back in the limelight. Control facilitates objective assessment of the real degree of vulnerability of the territory and the civil engineering works within it to take up the correct mitigation works in case of seismic events. The characteristics of innovative GPRs are particularly suitable in the field of civil protection activities, for example, in the management of post-seismic emergencies and geohazards, because the GPR not only ensures detailed and constant control but can also help law enforcement during forensic investigations.

The potential level of GPR sensitivity is very high. As illustrated here, even millimetric fractures can be detected by this non-destructive method. By increasing the frequency of the pulses, it is possible to have higher resolution and hidden, minute—even sub-millimetric—cracks can be detected in any type of building, whether modern or ancient [34]. The approach presented here should extensively

contribute to the development of specific and ad-hoc classification systems of the vulnerability of structures to earthquakes of various seismic power, within a general seismic classification [30,49].

References

1. Di Maggio, R.M.; Barone, P.M. (Eds.) *Geoscientists at Crime Scenes. A Companion to Forensic Geoscience*; Springer International Publishing: Heidelberg, Germany, 2017. [CrossRef]

2. Rivard, L.A. *Geohazard-Associated Geounits: Atlas and Glossary*; Springer Science & Business Media: Berlin, Germany, 2009. [CrossRef]

3. Busby, J.P.; Cuss, R.J.; Raines, M.G.; Beamish, D. *Application of Ground Penetrating Radar to Geological Investigations*; IR/04/21; British Geological Survey: Keyworth, UK, 2004; Available online: http://nora.nerc.ac.uk/11336/1/IR04021.pdf (accessed on 28 June 2018).

4. Gutiérrez, F.; Parise, M.; DeWaele, J.; Jourde, H. A review on natural and human-induced geohazards and impacts in karst. *Earth-Sci. Rev.* **2014**, *138*, 61–88. [CrossRef]

5. Borecka, A.; Herzig, J.; Durjasz-Rybacka, M. Ground penetrating radar investigations of landslides: A case study in a landslide in Radziszów. *Stud. Geotech. Mech.* **2015**, *37*, 11–18. [CrossRef]

6. Burton, I. Forensic disaster investigations in depth: A new case study model. *Environ. Mag.* **2010**, *52*, 36–41. [CrossRef]

7. International Strategy for Disaster Reduction (IRDR). *The FORIN Project*; IRDR: Bejing, China, 2011.

8. Anbazhagan, P.; Murali Krishna, A. Forensic investigation of earthquake induced failures during Sikkim 2011 earthquake, India. In Proceedings of the 15th Asian Regional Conference on Soil Mechanics and Geotechnical Engineering, Fukuoka, Japan, 9–13 November 2014; Japanese Geotechnical Society Special Publication: Tokyo, Japan, 2014. [CrossRef]

9. Takahashi, K.; Iitsuka, Y.; Koyama, C.N.; Sato, M. *Application of GPR CMP Measurements to Earthquake Diagnosis of Wooden Buildings*; International Symposium Non-Destructive Testing in Civil Engineering (NDT-CE): Berlin, Germany, 2015.

10. Nakasu, T.; Ono, Y.; Pothisiri, W. Forensic investigation of the 2011 Great East Japan Earthquake and Tsunami disaster: A case study of Rikuzentakata. *Disaster Prev. Manag. Int. J.* **2017**, *26*, 298–313. [CrossRef]

11. Woodward, J.; Stewart, I. Imaging near-surface tectonic structures using GPR: Western Eliki Fault, Gulf of Corinth, Greece. In Proceedings of the 12th International Conference on Ground Penetrating Radar, Birmingham, UK, 15–19 June 2008.

12. Rescue Radar. Available online: https://www.sensoft.ca/wp-content/uploads/2016/01/Forensic-Law-Enforcement_Search-Rescue_Buried-Victim-Search-Rescue.pdf (accessed on 28 June 2018).

13. Mitchell, J.K. Megacities and Natural Disasters: A Comparative Analysis. *GeoJournal* **1999**, *49*, 137–142. [CrossRef]

14. Yön, B.; Sayın, E.; Onat, O. *Earthquakes and Structural Damages*; InTech Open: Rijeka, Croatia, 2017. [CrossRef]

15. Jia, J.; Yan, J. Analysis about factors affecting the degree of damage of buildings in earthquake. *J. Phys. Conf. Ser.* **2015**, *628*. [CrossRef]

16. Smith, T.O.; Hoffman, S. (Eds.) *The Angry Earth: Disaster in Anthropological Perspective*; Routledge: New York, NY, USA, 1999. [CrossRef]

17. White, G.F.; Kates, R.W.; Burton, I. Knowing Better and Losing Even More: The Use of Knowledge in Hazards Management. *Glob. Environ. Chang. Part B Environ. Hazards* **2001**, *3*, 81–92. [CrossRef]

18. Mvududu, N.H.; Sink, C.A. Factor Analysis in Counseling Research and Practice. *CORE Counsel. Outcome Res. Eval.* **2013**, *4*, 75–98. [CrossRef]

19. Oliveira, C.S.; Ferreira, M.A.; Mota de Sá, F.; Bonacho, J. New Tools for the Analysis of the Generalized Impact of Earthquake Events. In *Earthquake Engineering and Structural Dynamics in Memory of Ragnar Sigbjörnsson*; Rupakhety, R., Ólafsson, S., Eds.; ICESD 2017; Geotechnical, Geological and Earthquake Engineering, 44; Springer: Cham, Switzerland, 2018. [CrossRef]

20. Villani, F.; Civico, R.; Pucci, S.; Pizzimenti, L.; Nappi, R.; De Martini, P.M.; Open EMERGEO Working Group. Data Descriptor: A database of the coseismic effects following the 30 October 2016 Norcia earthquake in Central Italy. *Sci. Data* **2018**, *5*, 180049. [CrossRef] [PubMed]

21. Chiaraluce, L.; Di Stefano, R.; Tinti, E.; Scognamiglio, L.; Michele, M.; Casarotti, E.; Cattaneo, M.; De Gori, P.; Chiarabba, C.; Monachesi, G.; et al. The 2016 Central Italy Seismic Sequence: A First Look at the Mainshocks, Aftershocks, and Source Models. *Seismol. Res. Lett.* **2017**, *88*, 1–15. [CrossRef]

22. Moretti, M.; Pondrelli, S.; Margheriti, L.; Mazza, S. SISMIKO: Emergency network deployment and data sharing for the 2016 central Italy seismic sequence. *Ann. Geophys.* **2016**, *59*, 8. [CrossRef]

23. Gruppo di Lavoro INGV sul Terremoto in Centro Italia. *Summary Report on the October 30, 2016 Earthquake in central Italy Mw 6.5*; INGV: Roma, Italy, 2016. [CrossRef]

24. ReLUIS-INGV Workgroug. Preliminary Study on Strong Motion Data of the 2016 Central Italy Seismic Sequence V6. 2016. Available online: http://www.reluis.it (accessed on 19 July 2018).

25. Pacor, F.; Paolucci, R.; Ameri, G.; Massa, M.; Puglia, R. Italian strong motion records in ITACA: Overview and record processing. *Bull. Earthq. Eng.* **2011**, *9*, 1741–1759. [CrossRef]

26. Liu, C.; Zheng, Y.; Xie, Z.; Xiong, X. Rupture features of the 2016 Mw 6.2 Norcia earthquake and its possible relationship with strong seismic hazards. *Geophys. Res. Lett.* **2017**, *44*, 1320–1328. [CrossRef]

27. Smeraglia, L.; Billi, A.; Carminati, E.; Cavallo, A.; Doglioni, C. Field- to nano-scale evidence for weakening mechanisms along the fault of the 2016 Amatrice and Norcia earthquakes, Italy. *Tectonophysics* **2017**. [CrossRef]

28. Everett, M. *Near-Surface Applied Geophysics*; Cambridge University Press: Cambridge, UK, 2014; ISBN 978-107018778.

29. Butler, D.K. (Ed.) *Near Surface Geophysics, Investigations in Geophysics 13*; Pristine Condition Like New edition; Society of Exploration Geophysicists: Tulsa, OK, USA, 2005; ISBN 978-1560801306.

30. Annan, A.P. *Ground Penetrating Radar: Principles, Procedures & Applications*; Sensors & Software, Inc.: Mississauga, ON, Canada, 2004.

31. Barone, P.M. *Understanding Buried Anomalies: A Practical Guide to GPR*; LAP-Lambert Academic Publishing: Saarbrucken, Germany, 2016; ISBN 978-3659935794.

32. Persico, R. *Introduction to Ground Penetrating Radar: Inverse Scattering and Data Processing*; Wiley-Blackwell: Oxford, UK, 2014; ISBN 9781118305003.

33. Jol, H.M. (Ed.) *Ground Penetrating Radar: Theory and Applications*; Elsevier: Amsterdam, The Netherlands, 2009.

34. Wai-Lok Lai, W.; Dérobert, X.; Annan, A.P. Review of Ground Penetrating Radar application in civil engineering: A 30-year journey from Locating and Testing to Imaging and Diagnosis. *NDT & E Int.* **2017**, *96*, 58–78. [CrossRef]

35. Binda, L.; Lualdi, M.; Saisi, A.; Zanzi, L. Radar investigation as a complementary tool for the diagnosis of historic masonry buildings. *Int. J. Mater. Struct. Integr.* **2011**, *5*, 1–25. [CrossRef]

36. Goodman, D.; Piro, S. GPR Imaging on Historical Buildings and Structures. In *GPR Remote Sensing in Archaeology*; Goodman, D., Piro, S., Eds.; Geotechnologies and the Environment; Springer: New York, NY, USA, 2013; Volume 9, pp. 143–157. [CrossRef]

37. Barone, P.M.; Di Matteo, A.; Graziano, F.; Mattei, E.; Pettinelli, E. GPR application to the structural control of historical buildings: Two case studies in Rome, Italy. *Near Surf. Geophys. EAGE* **2010**, *8*, 407–413. [CrossRef]

38. Pettinelli, E.; Barone, P.M.; Mattei, E.; Di Matteo, A. GPR application to historical buildings structural control. *Geophys. Res. Abstr.* **2009**, *11*, EGU2009-10382-1.

39. Barone, P.M.; Mattei, E.; Lauro, S.E.; Pettinelli, E. Non-destructive technique to investigate an archaeological structure: A GPR survey in the Domus Aurea (Rome, Italy). In Proceedings of the IEEE XIII International Conference on Ground Penetrating Radar (GPR 2010), Lecce, Italy, 21–25 June 2010. [CrossRef]

40. Kadioglu, S.; Kadioglu, Y.K. Picturing internal fractures of historical statues using ground penetrating radar method. *Adv. Geosci.* **2010**, *24*, 23–34. [CrossRef]

41. Ravaglioli, A. *Roma anno 2750 ab Urbe Condita. Storia, Monumenti, Personaggi, Prospettive, Roma*; Tascabili 1997; Newton Compton: Rome, Italy, 1997; ISBN 88-8183-670-X.
42. Diamanti, N.; Annan, A.P.; Redman, J.D. Concrete Bridge Deck Deterioration Assessment Using Ground Penetrating Radar (GPR). *J. Environ. Eng. Geophys.* **2017**, *22*, 121–132. [CrossRef]
43. Hugenschmidt, J. Concrete bridge inspection with a mobile GPR system. *Constr. Build. Mater.* **2002**, *16*, 147–154. [CrossRef]
44. Annan, A.P.; Redman, J.D. High speed ground-coupled GPR for road & bridge inspection. In Proceedings of the 11th International Conference on Structural Faults and Repair, Edinburgh, UK, 13–15 June 2006; p. 10.
45. Solla, M.; Lorenzo, H.; Rial, F.I.; Novo, A.; Riveiro, B. Masonry arch bridges evaluation by means of GPR. In Proceedings of the IEEE XIII International Conference on Ground Penetrating Radar (GPR 2010), Lecce, Italy, 21–25 June 2010. [CrossRef]
46. From Amatrice to Norcia to Rome, the Artistic Heritage Brought to Its Knees by the Earthquake. *La Repubblica*, 30 October 2016. (Italian Newspaper). Available online: http://www.repubblica.it/cronaca/2016/10/30/news/ferita_al_patrimonio_artistico_italiano-150904613/ (accessed on 2 July 2018).
47. Italy Earthquake Causes Cracks to Appear in St Paul's Basilica and Other Vatican landmarks. *The Independent*, 30 October 2016. (UK Newspaper). Available online: https://www.independent.co.uk/news/world/europe/italy-earthquake-today-rome-vatican-tourism-safety-pope-francis-st-paul-basilica-a7387861.html (accessed on 2 July 2018).
48. Italy Fears for Colosseum as 'Cracks Get Bigger' after Each Quake. *The Telegraph*, 31 October 2016. (UK Newspaper). Available online: https://www.telegraph.co.uk/news/2016/10/31/italy-fears-for-colosseum-as-cracks-get-bigger-after-each-quake/ (accessed on 2 July 2018).
49. Minghini, M.; Sarretta, A.; Lupia, F.; Napolitano, M.; Palmas, A.; Delucchi, L. Collaborative mapping response to disasters through OpenStreetMap: The case of the 2016 Italian earthquake. *Geoing. Ambient. Miner.* **2017**, *2*, 21–26.